Week 13

Ceramics and colloids

A. Testino

Sintering_2

References:

- J. Barton, P. Bowen, C. Carry & J.M. Haussonne - Les Céramiques. Les Traité des Matériaux, Volume 16, PPUR (2005)
- M.N. Rahaman - Ceramic processing and sintering. Taylor & Francis. Second edition (2003). Chapters 7-10
- A. Leriche, F. Cambier, S. Hampshire – Sintering of Ceramics. Reference Module in Materials Science and Materials Engineering (2017)
- M.G. Randal, P. Suri, S.J. Park – Review: liquid phase sintering. J.Mater. Sci. 44, 1-39 (2009)
- W. D. Kingery - Densification during Sintering in the Presence of a Liquid Phase. I. Theory, J. Appl. Physics, 30, 302-306 (1958)

Summary Week 12-13-14

1. Sintering fundamental (10)
2. Solid state sintering (16)
3. Grain growth & microstructure (22)
4. Liquid phase sintering (13)
5. Examples and practice (11)

Grain growth and microstructure: introduction

- The **properties** of the ceramics depend on the **microstructure**;
- The microstructure **evolves** during sintering. In particular:
  - Size, size distribution, and shape of the grains;
  - Amount of pores, their size and size distribution;
  - Nature and distribution of secondary phases.
- In general, for many applications, the microstructural control aims to achieve:
  - High (controlled) density; Small grain size; Homogeneous microstructure;
- The properties of the **sintered body** depend on the **green body**, which in turn depends on the powder quality!
- *Coarsening* is a competitive process to densification;
- Grain growth can be *normal* or *abnormal* ;

Normal and Abnormal grain growth

Normal grain growth: the grain size and shape occur within a relatively narrow range and the span of the grain size distribution is similar to that of an earlier time.

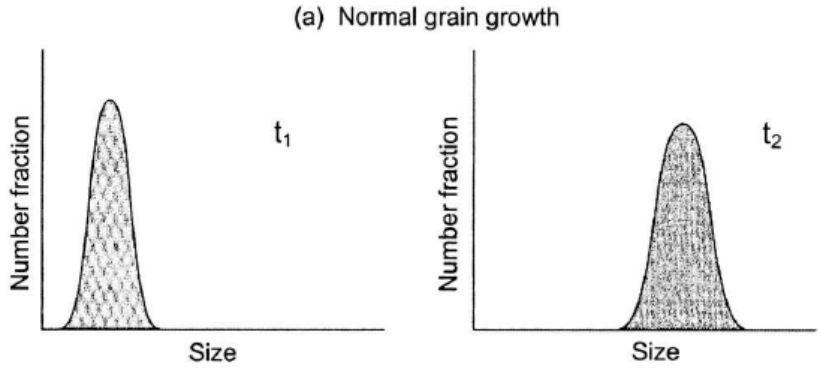

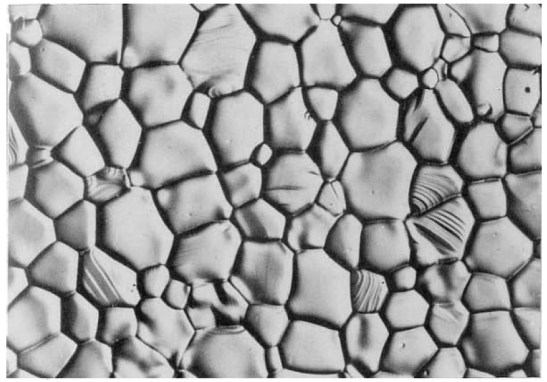

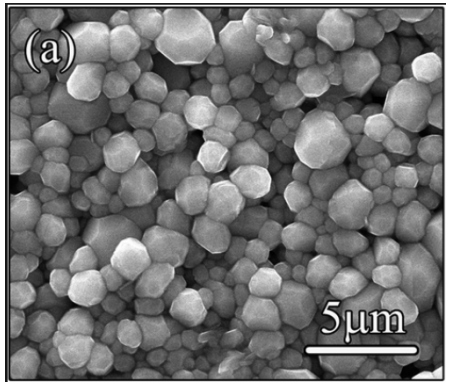

Abnormal (or exaggerated) grain growth: rapid growth of few larger grains at the expenses of the smaller ones.

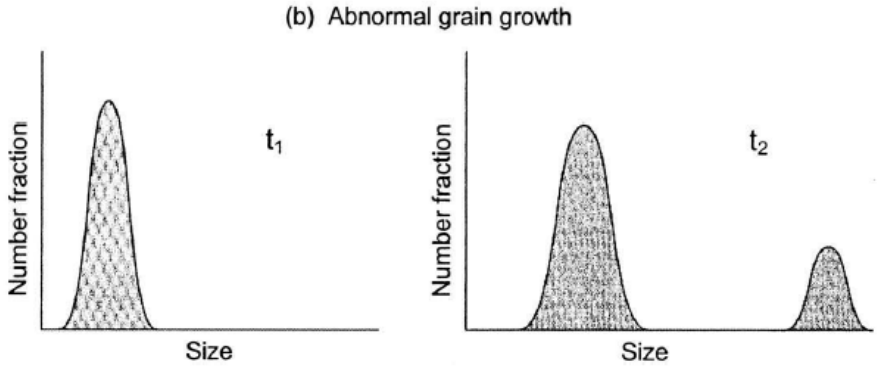

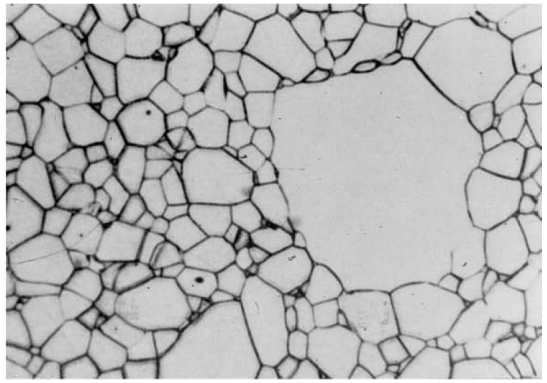

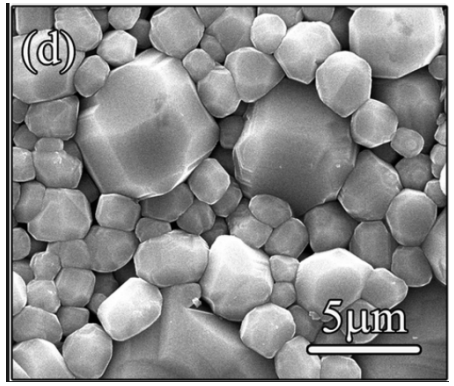

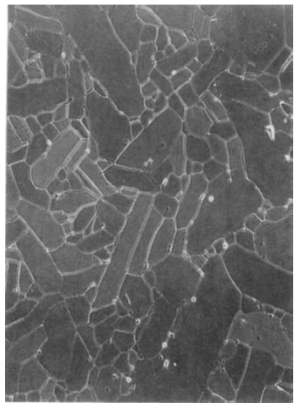

Anisotropic

Grain growth & driving force

The grain boundary is an extended 2D disordered region (extended defect, thickness 0.5-1 nm= 1-3 unit cells).

Atoms (or ions) diffuses less than an interatomic distance from one side to the other side of the GB. The GB moves and the grain grows.

As discussed before, the atoms moves from the *convex* to the *concave* surface because the difference in their chemical potential.

Therefore, the **GB moves towards its center of curvature**.

The driving force is always the same: surface decrease (GB area).

The surface term to consider is specific for that interface: γ_{gb} which is in the order of 0.2 – 1 J m^{-2}

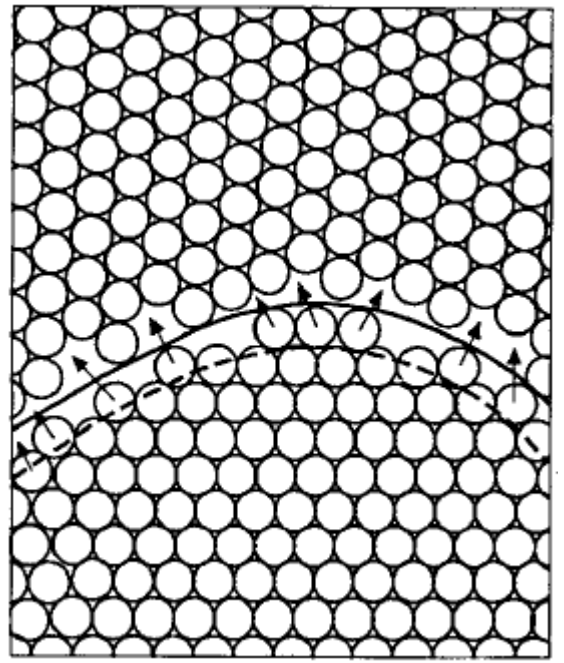

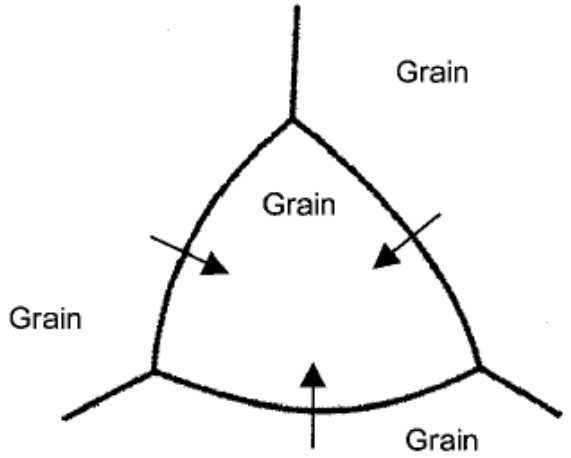

Grain size and properties

Generally, most properties are enhanced by smaller grain size: creep resistance (cold deformation upon stress) is an exception. The electrical and magnetic properties are affected by the grain size in a peculiar manner: the accurate control of the grain size allows the achievement of ceramics with tailored properties.
Example: ZnO, $BaTiO_3$

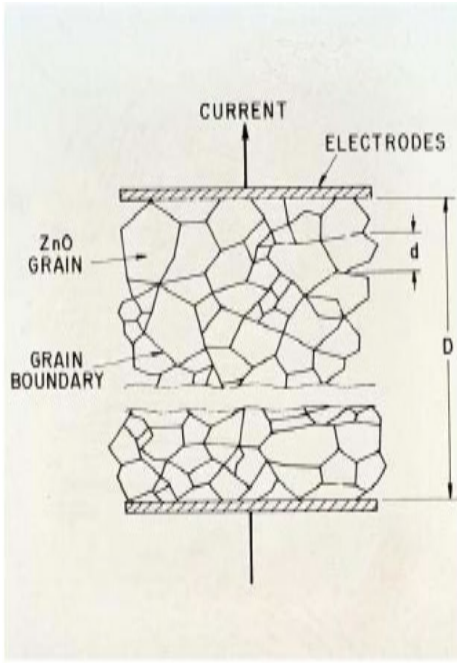

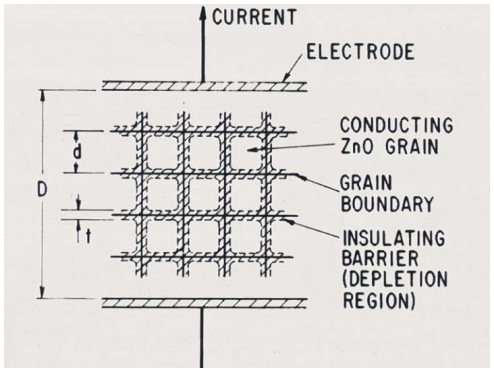

Brick-wall model

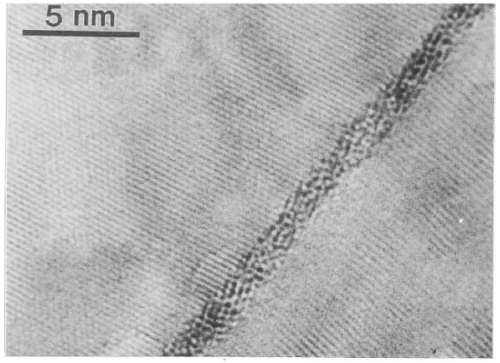

(c) $ZnO(Bi_2O_3)$: 1.5 nm

The breakdown voltage of varistor ceramics is directly proportional to the number of grain boundaries per unit of thickness and therefore to the inverse of the ZnO grain size.

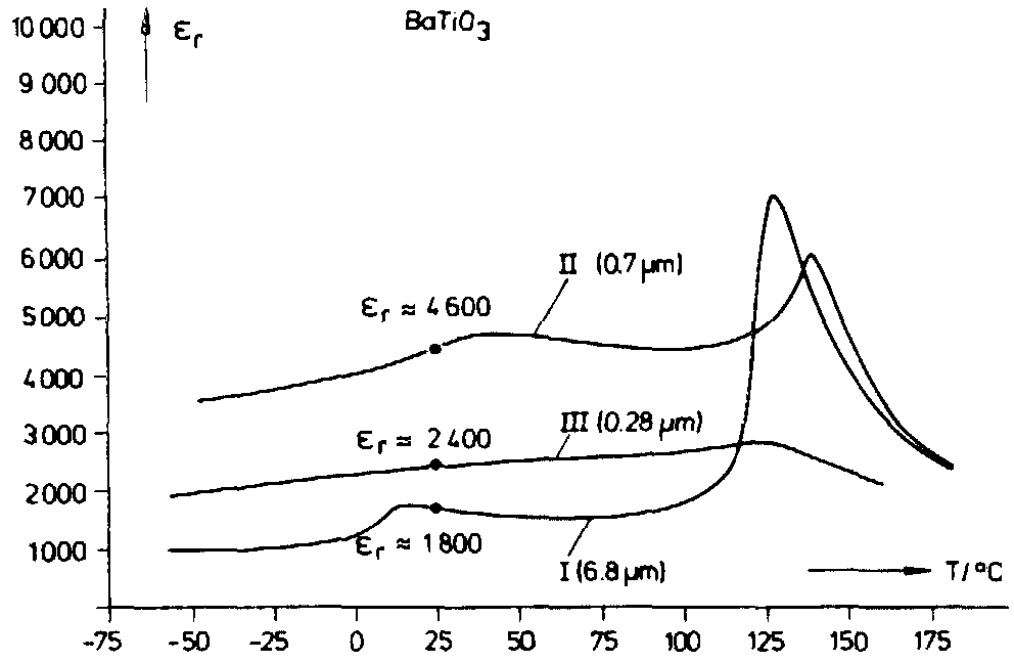

Dielectric constant vs. temperature of $BaTiO_3$ ceramic showing various grain sizes.

Toward full density

As discussed, for sintering by diffusion mechanisms: $\frac{1}{\rho}\frac{d\rho}{dt} = \frac{K(T)}{G^m}$

m=3 → lattice diffusion
m=4 → GB diffusion

Rapid densification requires short diffusion distances → grains have to be small

But the equation above shows that to a rapid grain growth a drastic reduction of densification rate corresponds. Therefore, a long sintering time is needed to achieve high density, which increase the possibility of abnormal grain growth to occur.

If abnormal grain growth occurs, pores can be trapped into large grains and their segregation will be almost impossible.

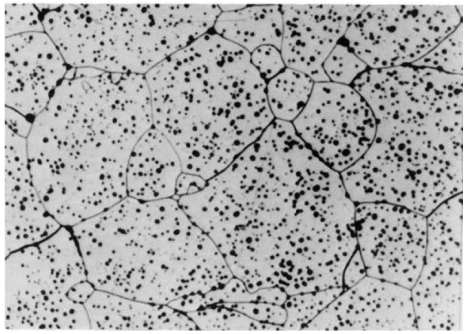

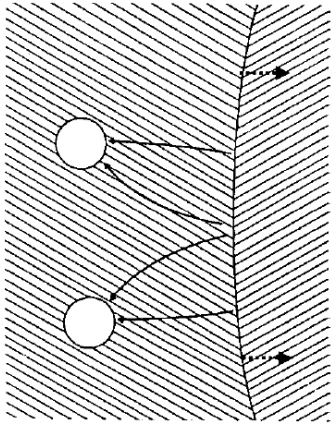

The attainment of high density requires control of **normal grain growth** as well as the avoidance of abnormal grain growth. Optimal sintering strategy, for a given green body, can be achieved based on the concept of the Master Sintering Curve (MSC, see section 5).

Normal grain growth

Model assumption: (1) the behavior of an isolated part of the GB is representative of the average behavior of the whole system; (2) the γ_{gb} is isotropic; (3) δ_{gb} is constant.

F_b: migration driving force
M_b: boundary mobility (which takes into account the migration mechanism)
α: geometrical constant (which takes into account the GB shape)

The GB velocity, v_b, is considered equal to the grain growth rate: $v_b \approx \frac{dG}{dt}$

And that the v_b can be represented as: $v_b = M_b F_b$

The pressure difference across the boundary: $\Delta P = \gamma_{bg}\left(\frac{1}{r_1} - \frac{1}{r_2}\right)$ (Young-Laplace eq.)

assuming that $\left(\frac{1}{r_1} - \frac{1}{r_2}\right) = \frac{\alpha}{G}$

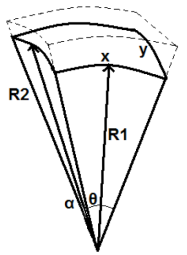

Remember:
2D surface

Normal grain growth

It results that:

$$v_b \approx \frac{dG}{dt} = M_b\left(\frac{\alpha\gamma_{bg}}{G}\right) \qquad M_b = \frac{D_a}{kT}\left(\frac{\Omega}{\gamma_{bg}}\right)$$

D_a: diff. coef. atom (limiting species)
G_0: grain size @ t=0
Q: activation energy for grain growth

$$G^2 - G_0^2 = K(T)t$$

$$K = 2\alpha\gamma_{bg}M_b = K_0\exp(-Q/RT)$$

Arrhenius-type equation: activated process

In practice, the grain growth data of dense polycrystalline solids do not follow the predicted law very well:

$$G^2 - G_0^2 = K(T)t \quad \Rightarrow \quad G^m - G_0^m = K(T)t$$

m: 2-4

In ceramics m=3 is common because of several diffusion mechanisms, as discussed, and segregation of impurities at the GB, etc.

Effects of dopants

A small amount of dopant (solute) is dissolved into the polycrystalline solid (host) (e.g., Sr in $BaTiO_3$). If the solute is attracted to (or repelled from) the GB, the solute ions will be nonuniform distributed in the GB region.

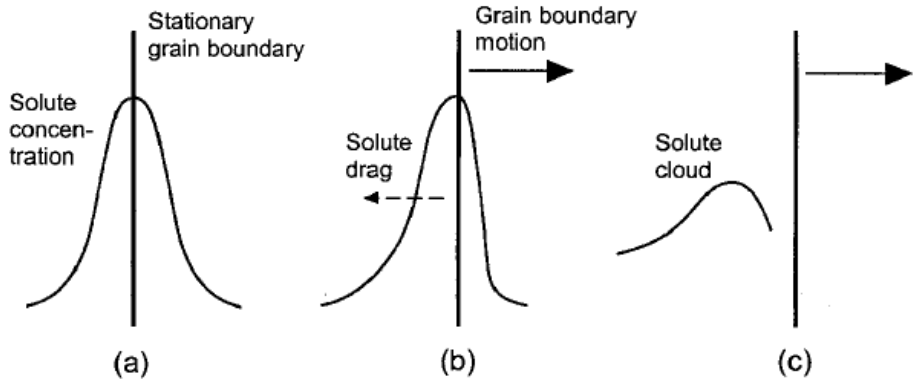

FIGURE 9.30 Sketch of the solute drag effect produced by the segregation of dopants to the grain boundaries. (a) Symmetrical distribution of the dopant in the region of a stationary grain boundary. (b) For a moving boundary, the dopant distribution becomes asymmetric if the diffusion coefficient of the dopant atoms across the boundary is different from that of the host atoms. The asymmetric distribution produces a drag on the boundary. (c) Breakaway of the boundary from the dopant leaving a solute cloud behind.

Two rates need to be compared: GB movement vs. dopant diffusion at the GB. In case (b) the GB motion is reduced (drag force).

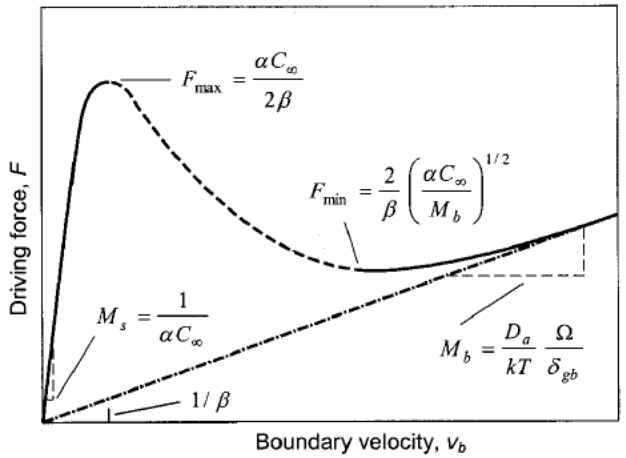

FIGURE 9.31 Driving force–velocity relationship for boundary migration controlled by solute drag and in the intrinsic regime. (From Ref. 44.)

Dopants and solubility limit

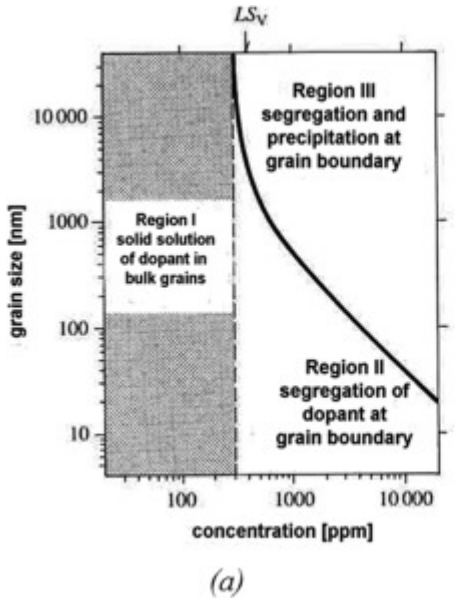

(a) Grain boundary segregation-precipitation for doped polycrystal vs. grain size and dopant content.

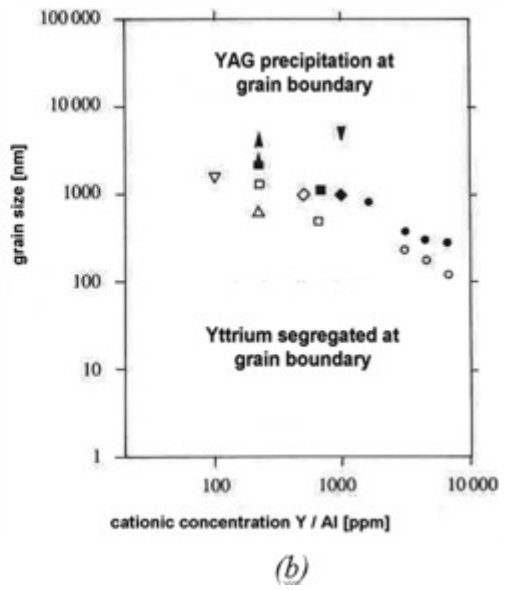

(b) Example of segregation of Y^{3+} at alumina grain boundaries (YAG=Y-Al Garnet) ($Y_3Al_5O_{12}$)

Dopants can be introduced to modify grain boundary energy.

When the concentration of the dopant is greater than the **solubility limit** in the major component, then **segregation occurs at grain boundaries** (region II).

Grain boundary **mobility is slowed** by segregated dopant ions.

Concentration of maximum dopant increases with surface to volume ratio of the grain, i.e., it is higher for nanosize grains.

Above a given concentration, a new (dopant-rich) phase precipitates.

Precipitation occurs at lower dopant concentrations as grain size increases. (region III).

Pinning effect (Zener model)

Let's assume a monosize, spherical, insoluble, immobile, and randomly distributed inclusions in a polycrystalline system. As usual, the driving force for GB movement is:

$$F_{gb} = \gamma_{gb}\left(\frac{1}{a_1} + \frac{1}{a_2}\right) \qquad \text{and assuming that } a_1, a_2 \propto \mathrm{G}$$

$$F_{gb} = \frac{\alpha\gamma_{gb}}{G}$$

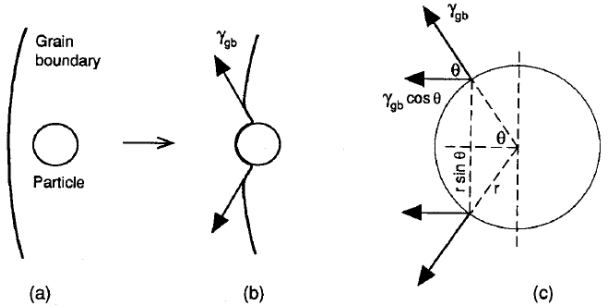

FIGURE 9.26 Interaction of a grain boundary with an immobile particle. (a) Approach of the boundary toward the particle. (b) Interaction between the grain boundary and the particle leading to a retarding force on the boundary. (c) Detailed geometry of the particle–grain boundary interaction.

F_{gb}: driving force (per unit of area) GB motion
G : grain size; a1, a2 (curvatures);
α: geometrical factor, α=2 for sphere
γ_{gb}: specific surface energy at GB
F_r: retarding force

The retarding force is: $F_r = (\gamma_{gb}\cos\theta)(2\pi r \sin\theta)$, which is max for θ=45° → $F_r^{max} = \pi r \gamma_{gb}$

For N_A (#) inclusions: $F_r^{max} = N_A \pi r \gamma_{gb}$ (per unit of GB area).

The number of inclusions per unit of volume is: $N_V = \frac{N_A}{2r}$ including the volume fraction of inclusion (f):

$$N_V = \frac{f}{(4/3)\pi r^3} \quad \rightarrow \quad F_r^{max} = \frac{3f\gamma_{gb}}{2r}$$

The net driving force: $F_{net} = F_{gb} - F_r^{max} = \gamma_{gb}\left(\frac{\alpha}{G} - \frac{3f}{2r}\right)$

When $F_{net} = 0$ the GB migration does not occur.

Therefore: $G_L = \frac{2\alpha}{3}\frac{r}{f}$ is the limiting grain size (Zener relationship).

Pinning effect

$$G_L = \frac{2\alpha}{3}\frac{r}{f}$$

Small grain size can be blocked (GB movement, grain growth) by smaller inclusions and by higher volume fraction of inclusions.
At **higher temperature** the equilibrium will be reached earlier in time.

Once the equilibrium is reached, grain growth will be inhibited unless:

- The inclusion changes size by coarsening;
- The inclusion may re-dissolved back into the lattice;
- Abnormal grain growth occurs.

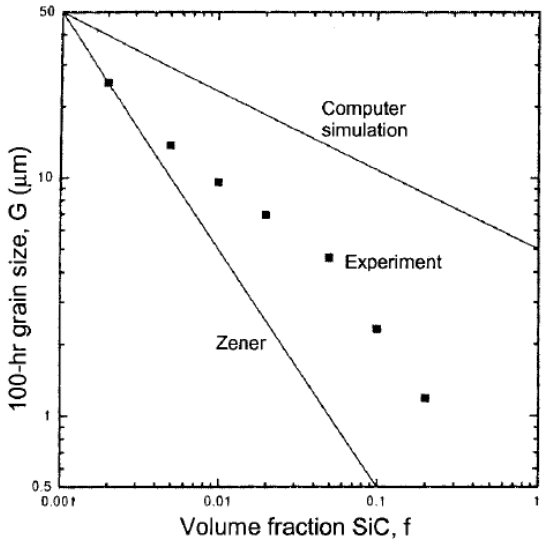

FIGURE 9.29 Data for grain size of Al_2O_3 (after annealing for 100 hour at 1700°C) as a function of SiC inclusion volume fraction, compared with the predictions of the Zener model and computer simulations. (From Ref. 60.)

Monte Carlo simulations have also performed with the attempts to predict the influence of pinning effect on grain growth. Experiments shows a relatively good agreement.

Examples

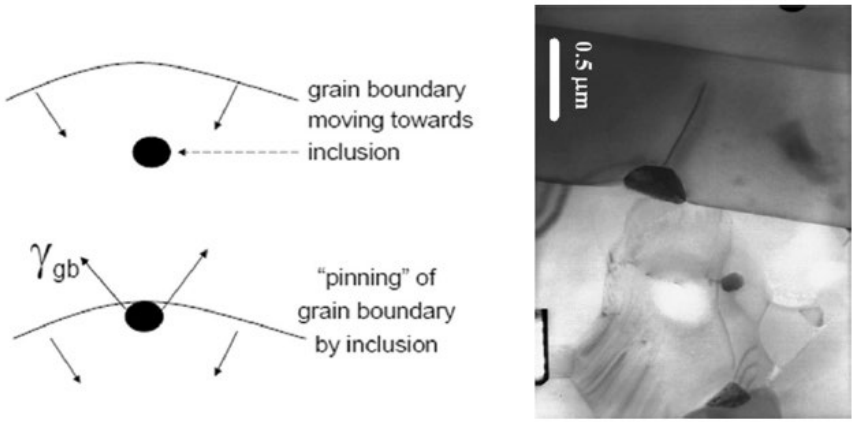

Fig. 36 Schematic illustration of effect of inclusion on grain boundary mobility (Petit, 2002).

Pinning effect

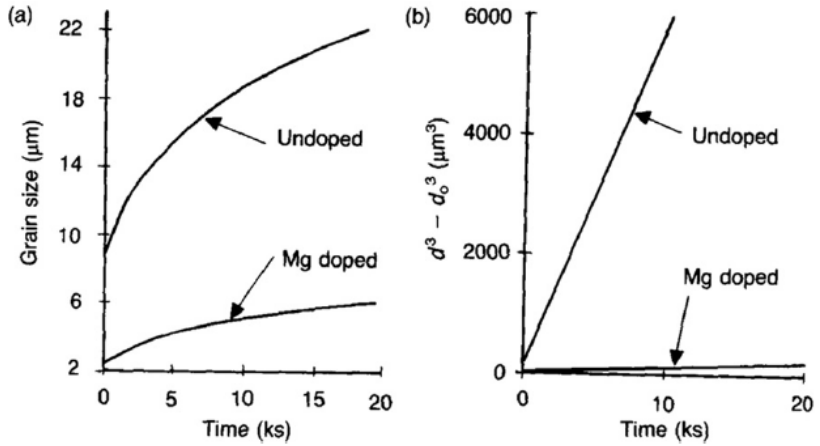

Fig. 34 Grain growth kinetic for pure alumina and MgO doped alumina (Lee and Rainforth, 1994).

Effects of dopants

Pore evolution (highly porous ceramics)

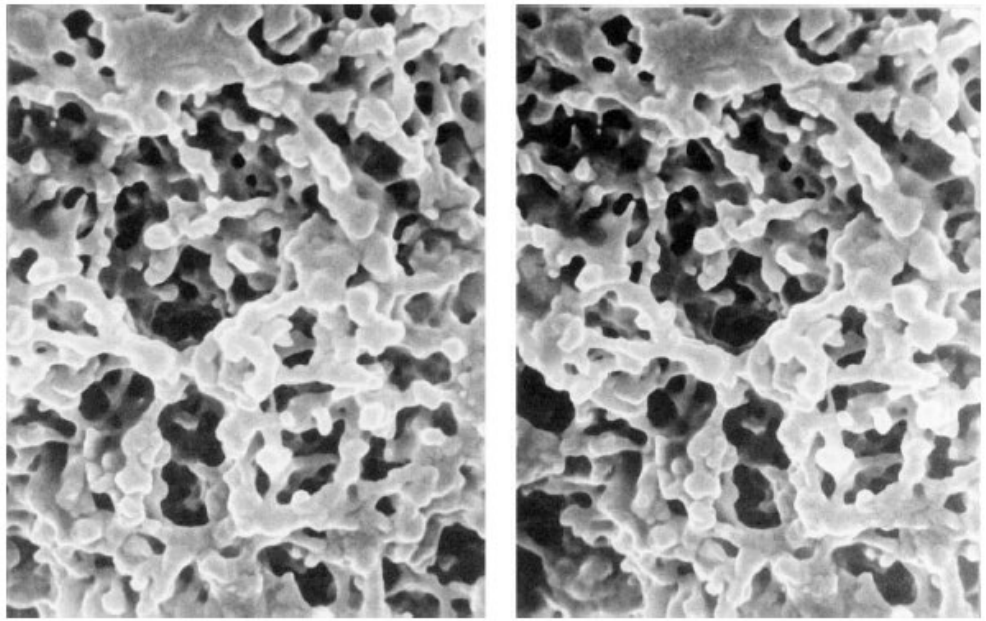

FIGURE 9.35 Stereographic pair of a replica of the pore space in a partially densified ZnO powder compact (density 73% of the theoretical). (Courtesy of M-Y. Chu.)

Epoxy resin forced into pores of ZnO and dissolution of the ceramics.

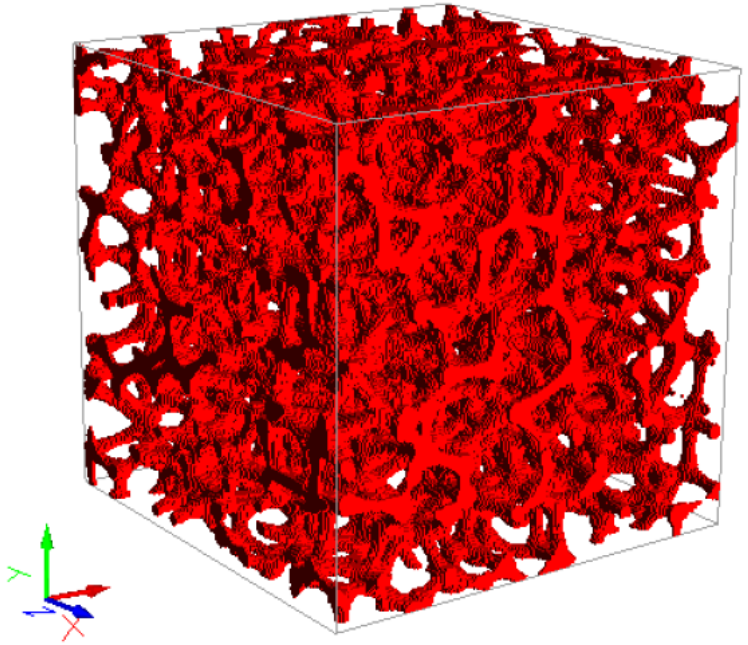

3D model of interconnected porosity. (Courtesy of W. Pabst)

Pore mobility (low porous ceramics)

Small isolated pores at the GB can be dragged along the GB movement.
Pore and GB are moving in the same direction: curvature of the surfaces.

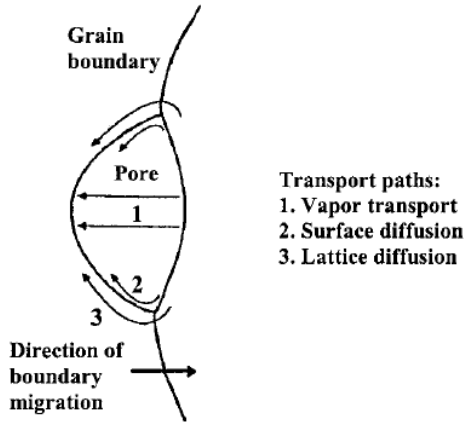

Pore under movement

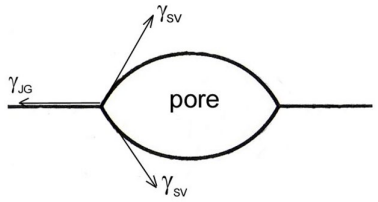

Equilibrium shape, not dragged

Two different scenario can be depicted:

(1) the pores remain at the GB and move with it (small pores). Pores have no effect on GB movement
Growth rate under *boundary control*

(2) the pores tend to be separated by the GB (large pores). Pores limit the GB movement.
Growth rate under *pore control*

Pore evolution

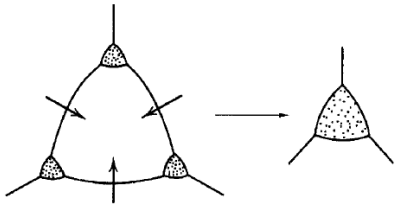

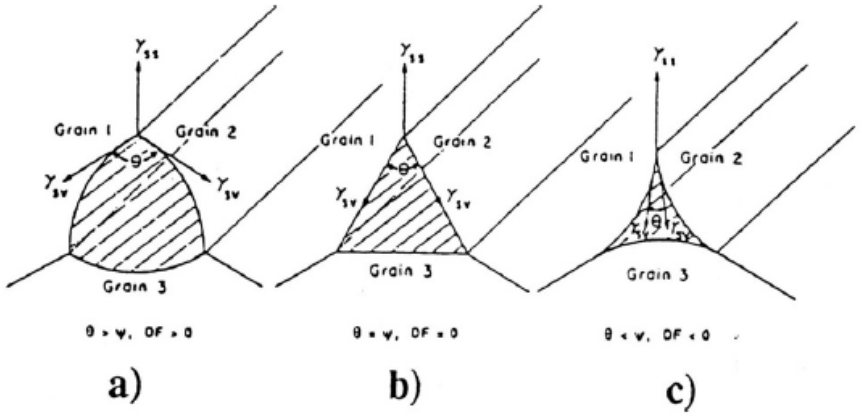

Fig. 16 Conditions for pore stability vs. dihedral angle. (a) Pore shrinkage, (b) pore stability, and (c) pore growth.

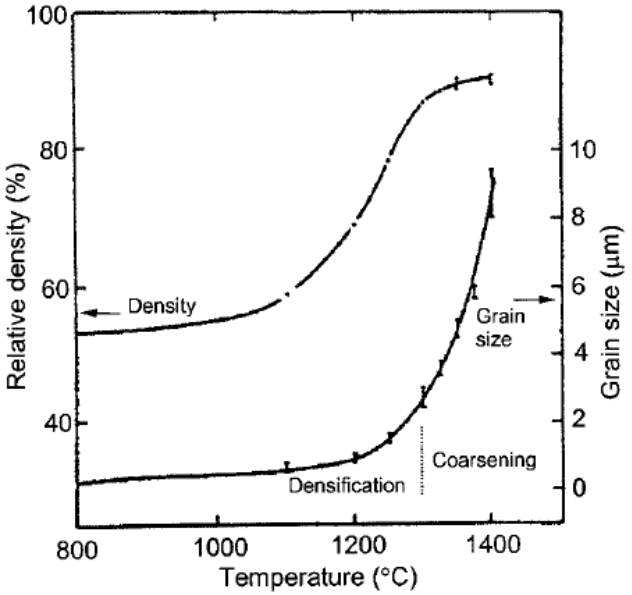

FIGURE 9.32 The density and grain size of a TiO_2 powder compact as a function of the sintering temperature. Rapid densification with limited grain growth occurs at lower temperatures followed by rapid grain growth with little densification at higher temperatures. (From ref. 73.)

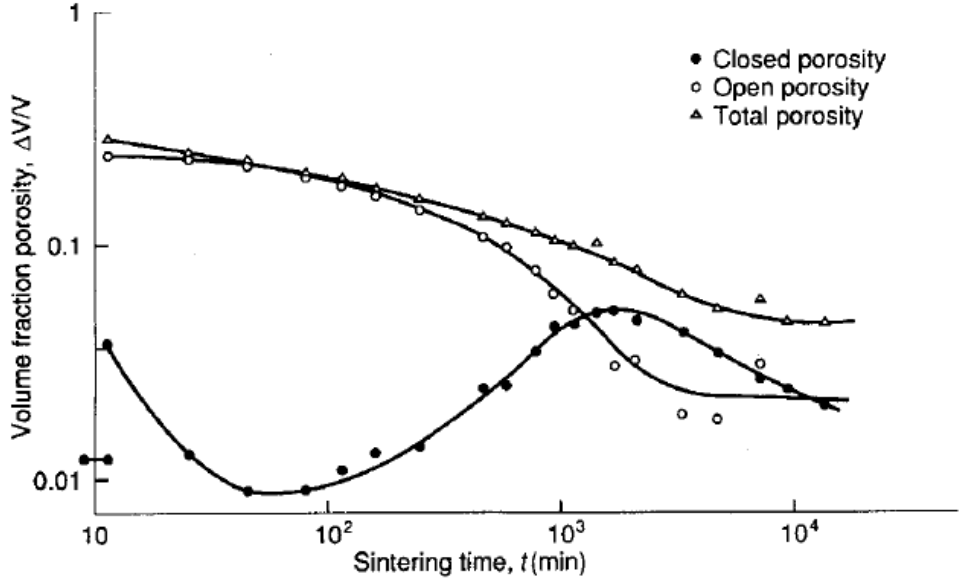

FIGURE 9.36 Change in porosity during the sintering of a UO_2 powder compact at 1400°C. (From Ref. 76.)

Grain growth (coarsening)

TABLE 9.3 Grain Growth Exponent m in the Equation $G^m = G_0^m + Kt$ for Various Mechanisms

Mechanism[a]	Exponent m
Pore control	
Surface diffusion	4
Lattice diffusion	3
Vapor transport (vapor pressure p = constant)	3
Vapor transport ($p = 2\gamma_{sv}/r$)	2
Boundary control	
Pure system	2
System containing second-phase particles	
Coalescence of second phase by lattice diffusion	3
Coalescence of second phase by grain boundary diffusion	4
Solution of second phase	1
Diffusion through continuous second phase	3
Doped system	
Solute drag (low solubility)	3
Solute drag (high solubility)	2

[a]The pore control kinetics are given for the situation where the pore separation is related to the grain size, i.e., the number of pores per unit area of the boundary $N_A \sim 1/G^2$. Changes in distribution during growth would change the kinetics.

Densification and coarsening, at least in the final stage of sintering, occurs simultaneously, influencing each other. Both processes are complicated, only qualitative consideration on their interaction can be outlined. Considering the generalized equation

$$G^m = G_0^m + Kt$$

a rough idea of the dominating coarsening mechanism may be argued.

Densification and coarsening

G: grain size
2r: pore size

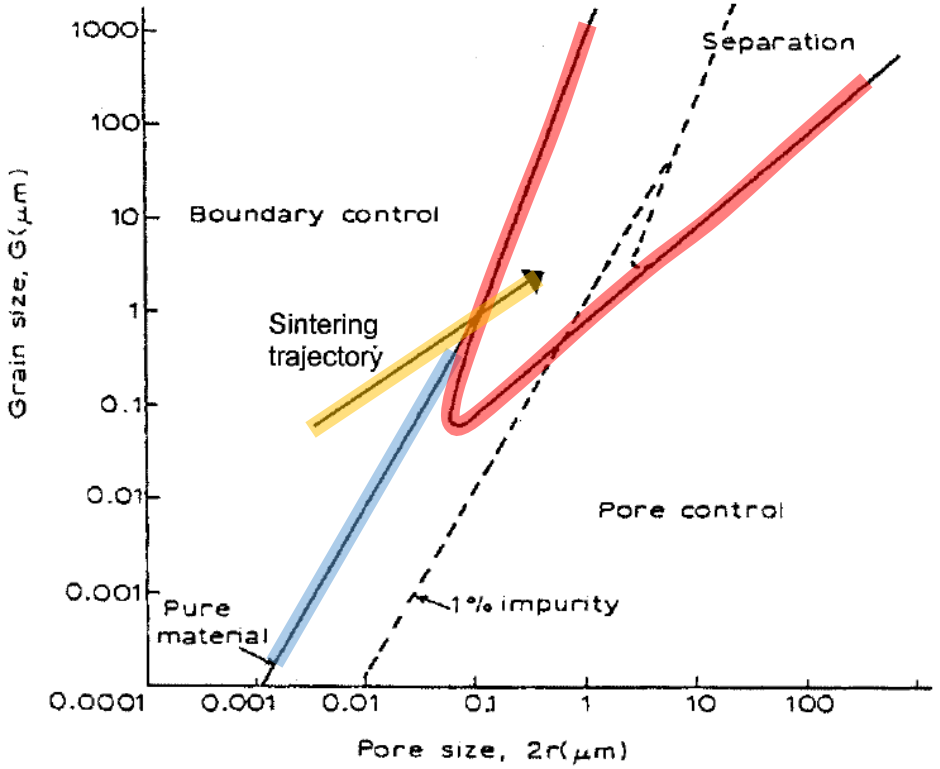

FIGURE 9.47 The dependence of the type of pore-boundary interaction on microstructural parameters when pores migrate by surface diffusion. The interpore spacing is assumed to be equal to the grain size. (From Ref. 83.)

As discussed, two limiting cases: *pore* (large pores) or *boundary* (small pores) control.
A real sample has large and small pores.

Large pores are less mobile and control the motion.
Small pores are more mobile and move with the GB.
These two conditions are separated by a curve, the *equal mobility curve* (light blue line).

The *separation curve* (light red curve) identify the separation area where two processes are in competition and abnormal grain growth can occur.

The yellow line depict the sintering profile: the separation zone should be avoided to achieve high density with controlled grain size. The effect of dopants is also indicated (see slides #10)

Densification and coarsening

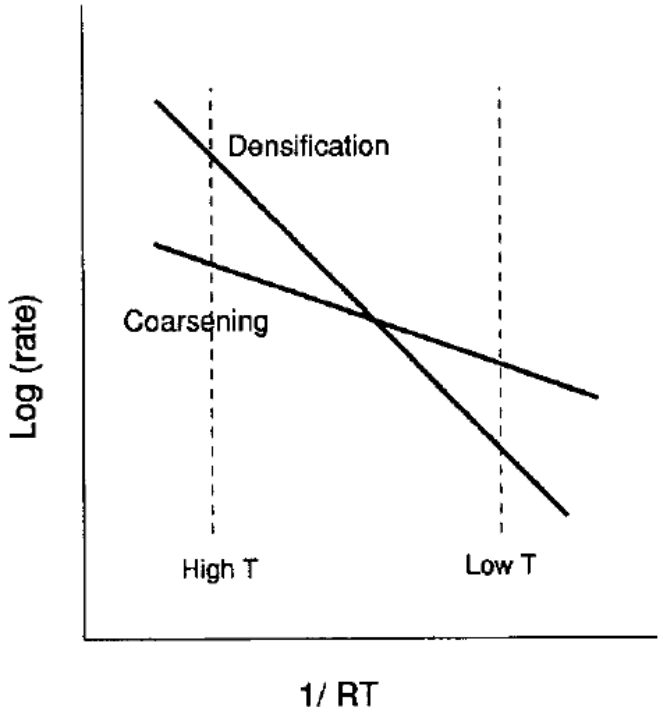

FIGURE 9.52 Under conditions where the densification mechanism has a higher activation energy than the coarsening mechanism, a fast heating rate to high firing temperatures (fast firing) can be beneficial for the achievement of high density.

An optimal sintering strategy needs to be identified for each case. The master sintering curve (MSC) approach can help but the identification of the optimal sintering protocol for a defined application remains (almost) an art!

Remarks of the section

- Different equation describing the kinetics of **normal** and **abnormal** grain growth exist;
- This model considers an **isolated GB** or a single grain, therefore only **qualitative** assessment;
- A considerable gap exists between the **theoretical** understanding of the microstructural evolution and **real** cases. However, **guide lines** can be identified;
- High density coupled with controlled grain is achievable if **coarsening is mitigated** and **abnormal** grain growth **avoided**;
- **Pore management** is the key to achieve high density ceramics;
- Solid –state sintering **has limitation.** In some cases, liquid phase sintering might be effective;
- **Properties** depend on microstructure. Final microstructure depends on thermal history and green properties. Green properties depends on forming methods and **powder quality.**

No good powders = No good ceramics!

Liquid Phase Sintering: introduction

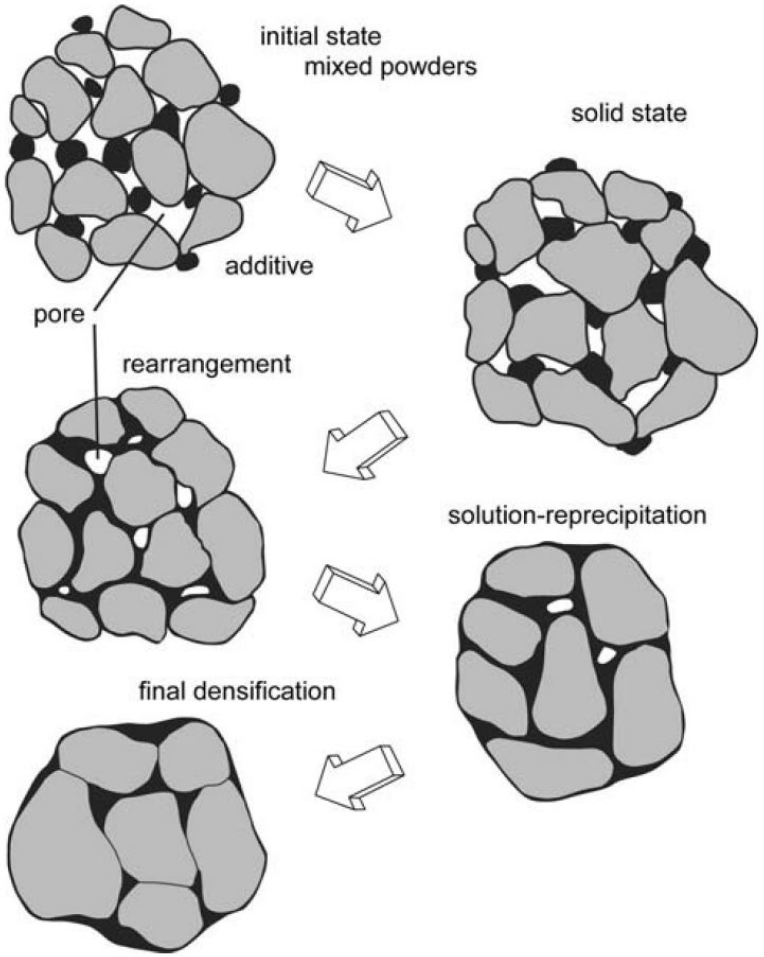

Fig. 1 A schematic of the microstructure changes during LPS, starting with mixed powders and pores between the particles. During heating the particles sinter, but when a melt forms and spreads the solid grains rearrange. Subsequent densification is accompanied by coarsening. For many products there is pore annihilation as diffusion in the liquid accelerates grain shape changes that facilitates pore removal

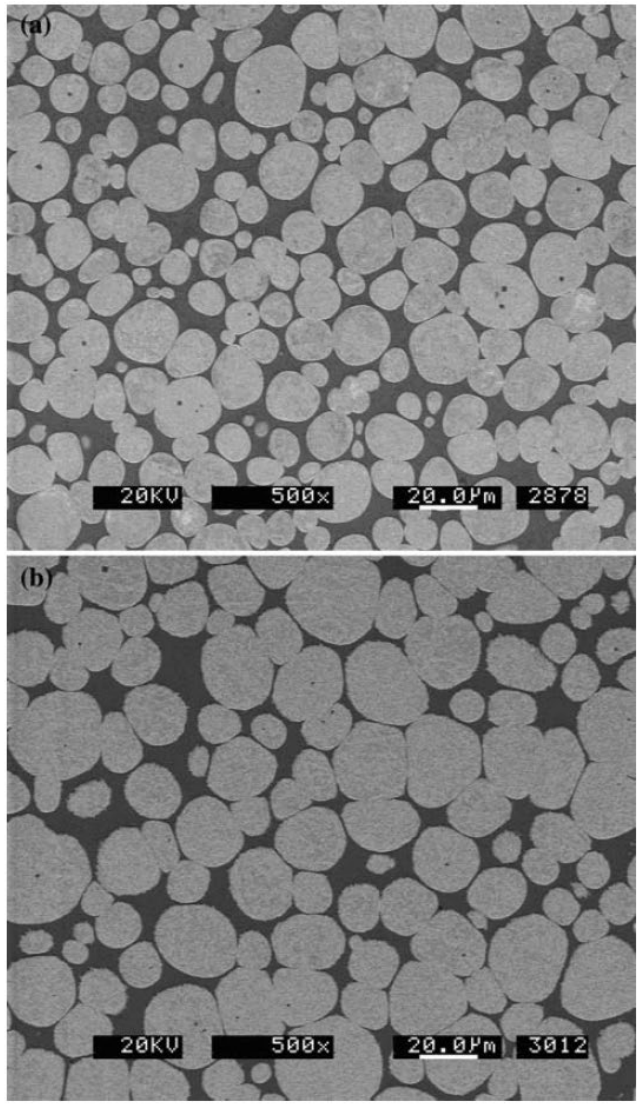

Fig. 4 These two micrographs of a 88 wt.% W heavy alloy with 15.4 wt.% Ni and 6.6 wt.% Fe were taken after two different hold times at 1500 °C, **a** 0 min and **b** 30 min. The structure is well developed by the time the sintering temperature is reached and the structures are similar except for a longer length scale with the longer time

- LPS is a process for high performance, *multiphase* components from powders;
- Sintering occurs under conditions where solid grains *coexist* with a wetting liquid;
- *Wettability* is a key concept;
- LPS is the *dominant commercial* sintering process: the final product is a composite with customized properties;
- The liquid phase may be a *viscous glass*;
- Several composite can be obtained , including *cermet* (e.g. TiC-Fe);
- LPS may be use to densify materials that *cannot be fabricated* using other manufacturing approach (e.g. WC/Co, eutectic @ 1310, drilling and cutting tools;
- At the sintering temperature the solid can be soluble in the liquid phase (*persistent* LPS);
- On cooling the liquid solidifies to produce a composite microstructure with *tailored* properties.

Liquid Phase Sintering: examples

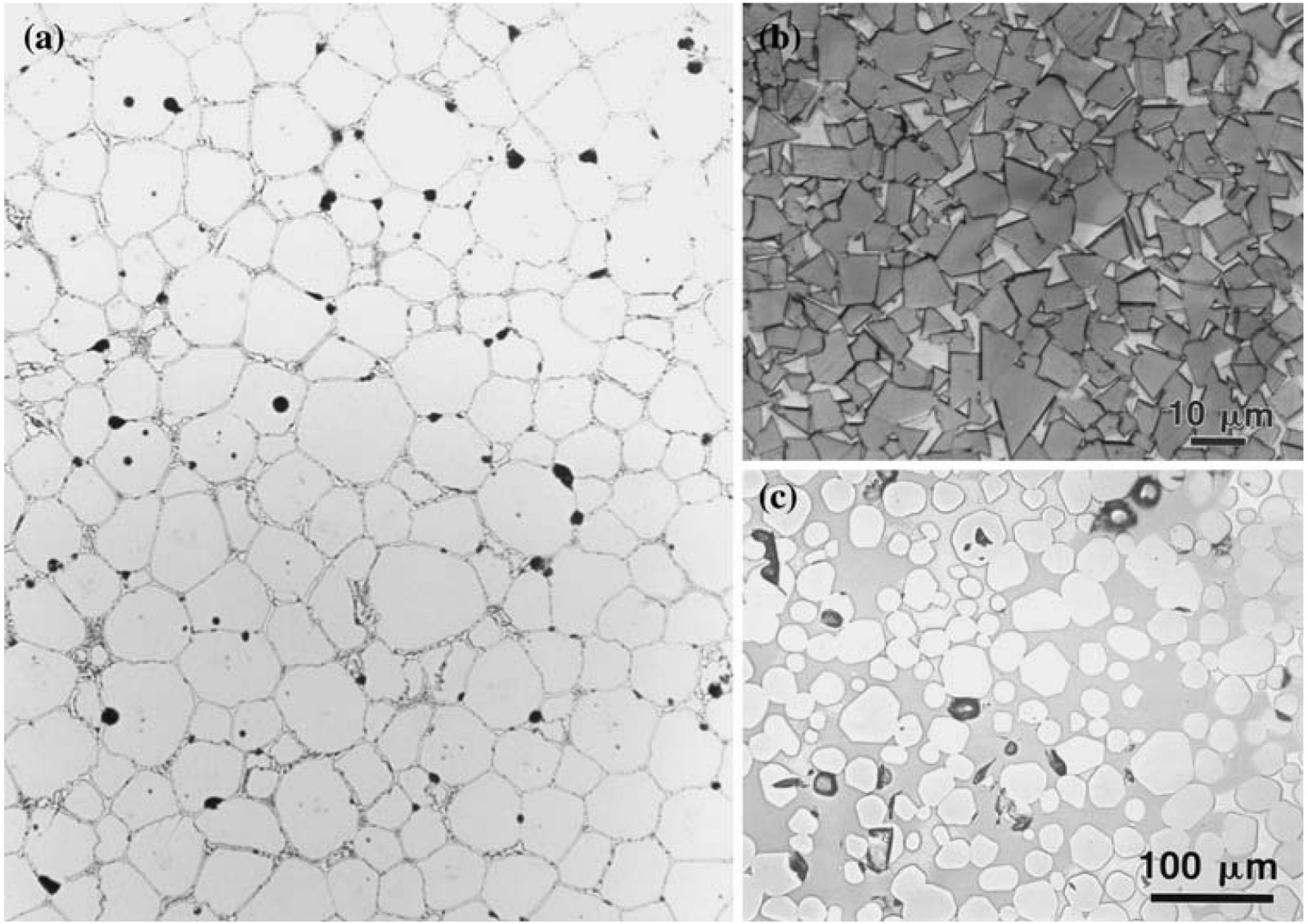

Three example microstructures after LPS: a) tool steel, b) cemented carbide, and c) molybdenum disilicide–copper composite

Wettability and spreading

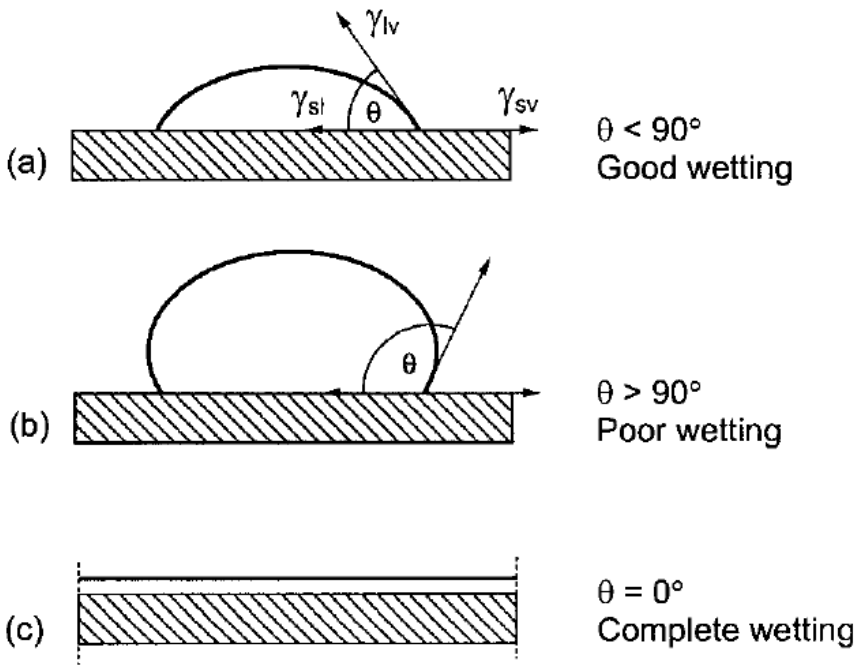

FIGURE 10.4 Wetting behavior between a liquid and a solid showing (a) good wetting, (b) poor wetting, and (c) complete wetting for a liquid with a contact angle of θ.

- In general, liquids with low surface tension readily wet most solids, giving a low contact angle, θ.
- At molecular level, it is a matter of **cohesion** and **adhesion**: if the **cohesion** between the liquid molecules is **greater than adhesion** between the liquid and the solid, the liquid will **not** want to wet the solid (see adhesion/cohesion energy in lesson 4-5).
- It is a three phase system: gas-liquid-solid. Three interfacial energies:

$$\gamma_{sv} = \gamma_{sl} + \gamma_{lv} \cos\theta$$ Young-Dupré

- Spreading: $\gamma_{lv} + \gamma_{sl} - \gamma_{sv} = 0$

Stages of LPS

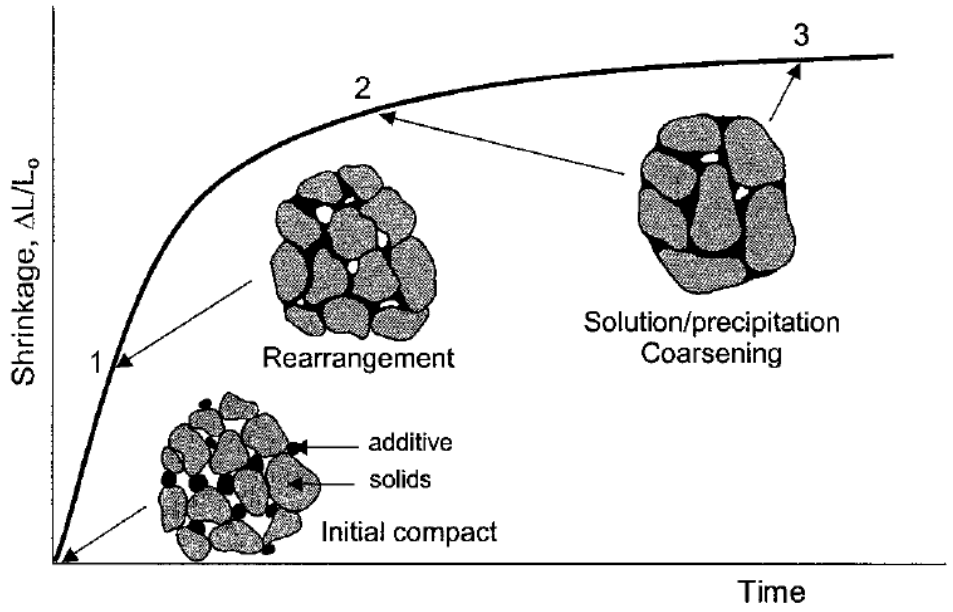

FIGURE 10.3 Schematic evolution of a powder compact during liquid-phase sintering. The three dominant stages overlap significantly.

Additive: sintering aid

1. Redistribution of the liquid and *rearrangement* of the particulate solid under the influence of the capillary force;
2. Densification and grain shape accommodation by s*olution-precipitation* (Ostwald ripening, coarsening);
3. *Final stage sintering* driven by the residual porosity in the liquid.

Before the formation of the liquid phase **solid-state sintering** may occur, with an initial densification.

The **capillary force** of the liquid phase produce a high packing density.

Because of the solubility of the solid phase, the **sharp edges** of the solids particles are **preferentially dissolved**, leading to particles with **smooth surface** (in case of small amount of liquid phase, faceting may occur)

Driving force

Let's consider the forces acting on the multiphase system:

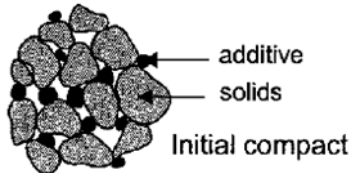

Interaction s-s, s-v, l-v, s-l

The wetting condition: $\gamma_{sv} > \gamma_{lv} > \gamma_{ss} > 2\gamma_{sl}$

As soon as the liquid melts, it coats the solid, and s/v (and s/s) interface disappears. Pores (v) in the liquid are formed. The (negative) pressure inside the pores is:

$$P^0 = \frac{-2\gamma_{lv}}{r_p}$$

which is higher than that of the liquid and it generates a compressive capillary stress that is equivalent to placing the entire system under an equivalent hydrostatic pressure.

The **driving force** leading to densification is the decrease of this l/v surface area (overall decrease of surface energy).

Example: 500 nm pores in silica at 1400 °C, γ_{lv} =0.85 J m^{-2}

$$P^0 = \frac{-2\gamma_{lv}}{r_p} = \frac{2 \times 0.85[J\ m^{-2}]}{0.5\ 10^{-6}[m]} = 3.4\ 10^6[N\ m^{-2}] = 34\ \text{bar}$$

Capillary force and rearrangement stage

The capillary pressure hold together the particles, and the thin viscous layer between the particle allows their rearrangement toward the maximum packing density.

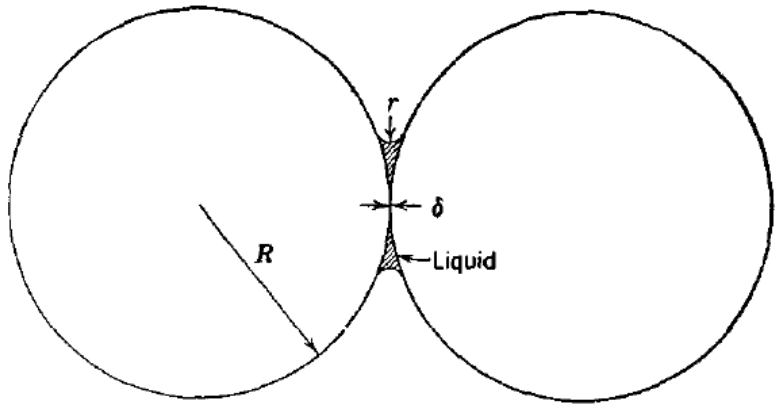

However, if particles do not change shape (unless a huge amount of liquid phase is present), full densification cannot be achieved (limit: packed spheres).

The size of the pores decrease (higher capillary force) but the densification rate can be approximated to a viscous flow:

$$\frac{\Delta L}{L} = \frac{1}{3}\frac{\Delta V}{V} \approx t^{(1+y)}$$

where y>0 (and depends on T). The increase in driving force is counteracted by the viscous flow.

Capillary force and rearrangement stage

The sphere do not come into contact, a thin liquid film (δ) remains at the interface, as a results of repulsive force between particles.

The capillary force is balanced by compressive force. This pressure results in an increase of the local chemical potential:

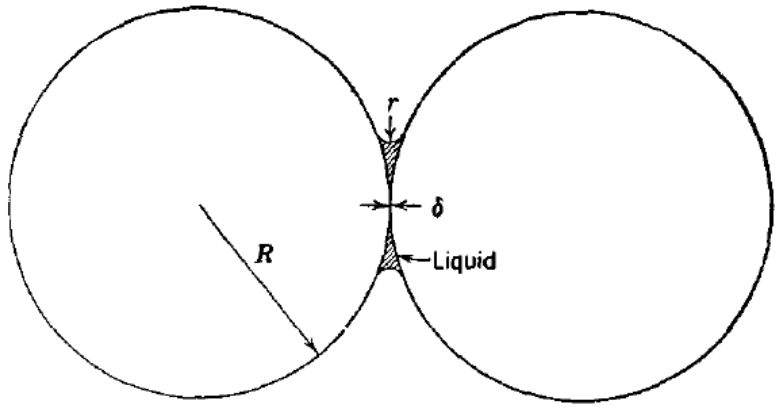

$$\mu - \mu_0 = RT \ln\left(\frac{a}{a_0}\right) = \Delta P V_0 \qquad \ln\left(\frac{a}{a_0}\right) = \frac{K 2\gamma_{lv} V_0}{r_0 RT}$$

K: constant relating the maximum contact area pressure to the overall hydrostatic pressure

The activity at the contact points is increased and provides a **driving force** for transferring material in such a way that the particle centers can move together and the density increase.

The major change in free energy that takes place during densification is due to the *decrease in surface area of pores in the liquid phase*, and this provides the *driving force for sintering*.

Rearrangement and liquid phase fraction

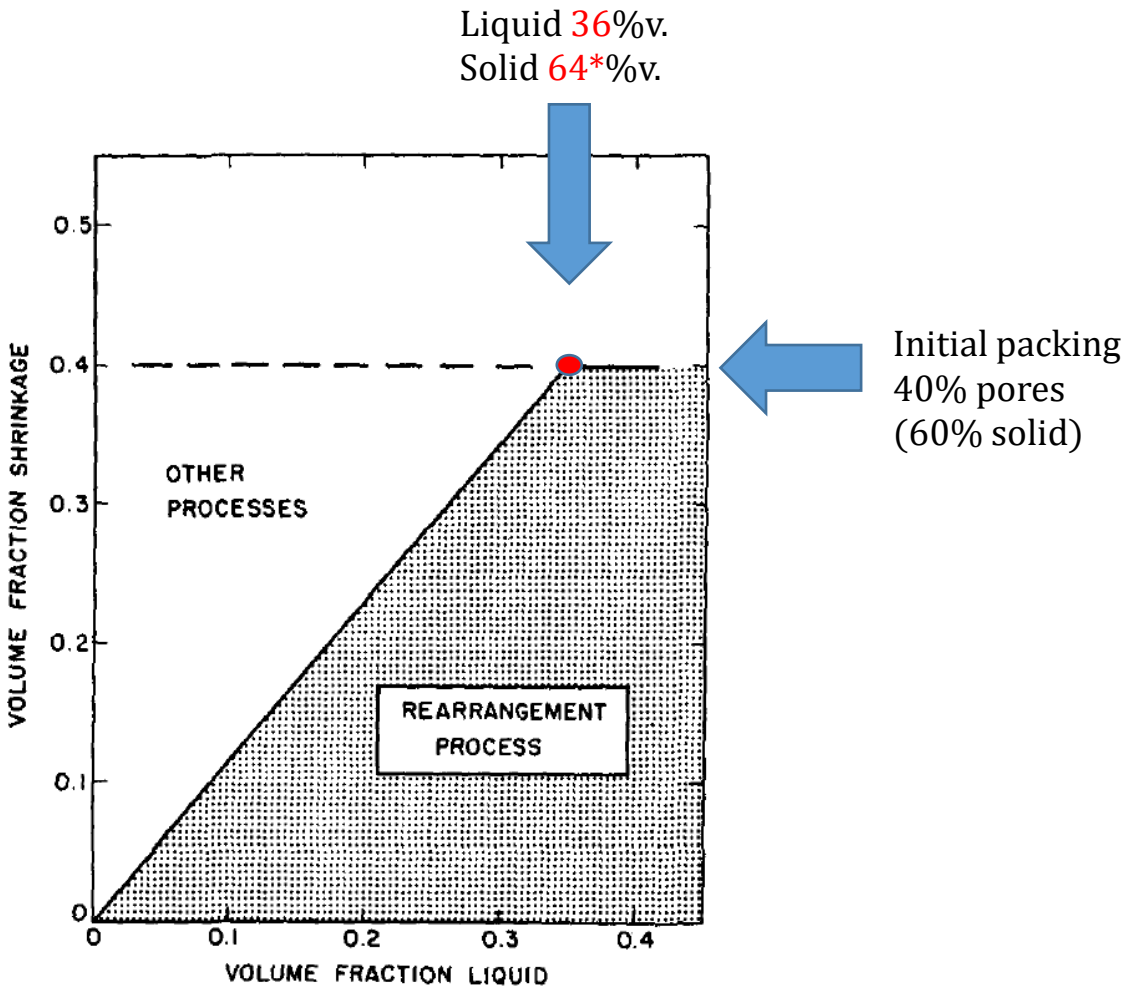

FIG. 3. Fractional shrinkage due to the "rearrangement" process with different liquid contents.

Fig 10.25 of Rahaman's book

- Initial packing: 40%v. (typical value)
- Liquid phase after melting occupy 35%v. volume of the final compact, full density by pure rearrangement is achievable (red spot).
- This value is close to that for dense random packing of monosize sphere (the space among spheres is occupied by the liquid phase)
- For smaller amounts of liquid, the fractional decrease in volume which can take place by rearrangement is somewhat less.
- To achieve high density, some additional sintering process is necessary.

*dense random packing of monosize spheres

Simulation

Monte Carlo Simulation (MCS)

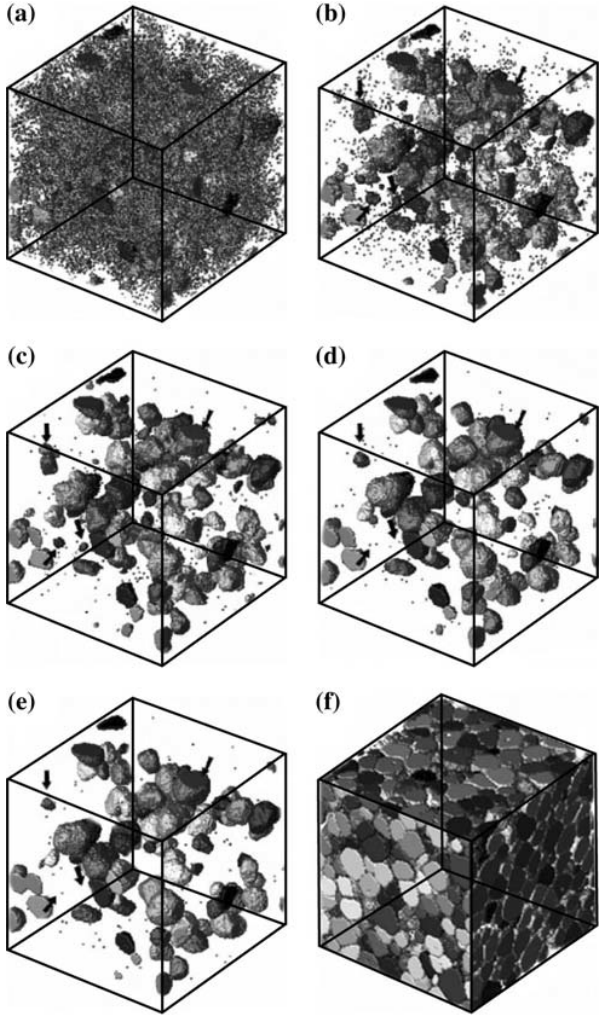

Fig. 56 Temporal evolution of a simulated 3D microstructure with an initial solid fraction of 0.7. The snapshots were obtained at **a** 6000, **b** 12000, **c** 24000, **d** 120000 and **e** and **f** 200,000 Monte-Carlo steps (MCS). To improve visualization, the liquid is not shown. In addition, to illustrate the coarsening process more effectively only a portion of the grains are shown from **a** to **e**. Coarsening occurs with the larger grains growing at the expense of smaller grains (marked with *arrows*) [194]

Discrete Element Method (DEM)

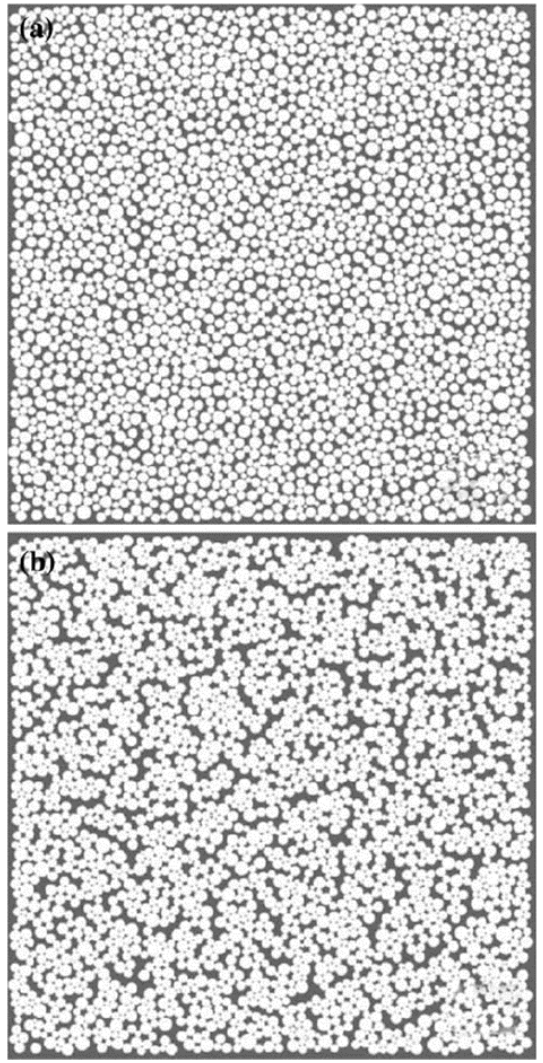

Fig. 57 A two-dimensional DEM simulation of grain rearrangement during the early portion of LPS: **a** starting structure with a relative density around 0.65 and **b** simulation of rearranged structure due to viscosity [205]

Solution precipitation stage

Particles rearrangement has occurred and a thin film of liquid phase is compressed among the particles. At the contact point the solubility is larger (higher potential): a gradient is established and a diffusive mass transfer away form the contact point occurs. The particle center-to-center distance decreases and densification takes place.

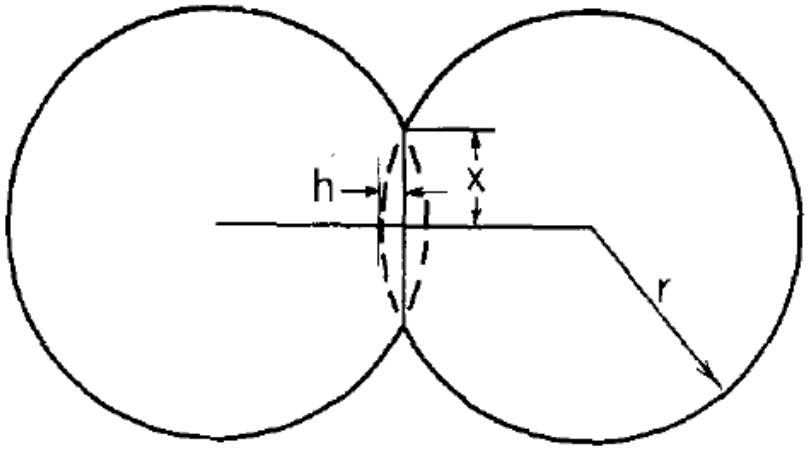

FIG. 4. Spheroidal particles approach due to solution at the contact area.

As usual, an approximated geometrical model is needed.

$$h = \frac{x^2}{2r} \qquad V = \frac{\pi x^2 h}{2} = \pi r h^2$$

V: volume of removed matter

Matter flow by diffusion: $J = 4\pi D \Delta C$ through the film δ

$$\frac{dV}{dt} = J\delta = 4\pi\delta D(C - C_0)$$

The concentration gradient depend on the pressure at the contact point. We need a relationship between pressure and particles and pores size.

Solution precipitation stage

First, a relationship between pore size (r_p) and particle size (r_s): $r_p = \left(\frac{V_s}{V_p}\right)^{1/3}$ $r_p = k_1 r_s$

And then, it is reasonable to assume that the pressure at the contact area is inversely proportional to the ratio of the contact area to the projected particle area:

$$\Delta P = \frac{k_2}{(x^2/r^2)} P^0 = \frac{k_2 r^2}{2rh}\left(\frac{2\gamma_{lv}}{r_p}\right) = \frac{k_2 \gamma_{lv}}{k_1 h} \qquad \mu - \mu_0 = RT \ln\left(\frac{a}{a_0}\right) = \Delta P V_0$$

where k_2 is a proportionality constant. Concentration gradient is:

V_0: initial volume

$$(C - C_0) = C_0 \left[\exp\left(\frac{k_2 \gamma_{lv} V_0}{k_1 hRT}\right) - 1\right]$$

To a decrease of the volume, a decrease of pore volume corresponds:

$$\Delta V = \frac{4}{3}\pi\left(r_{p0}^3 - r_p^3\right) = \frac{\pi x^4}{16r} \quad \Rightarrow \quad r_P = \left(r_{p0}^3 - \frac{3x^4}{64r}\right)^3$$

For x: 0→ 0.4 (+40%)
r_p: 1→ 0.94 (-6%)

Solution precipitation stage

The decrease in volume of the particles must be equal the flux of matter from the circumference of the circular contact area:

$$\frac{dV}{dt} = 4\pi\delta(C - C_0) = 4\pi D\delta C_0 \left[\exp\left(\frac{k_2\gamma_{lv}V_0}{k_1 hRT}\right) - 1\right] = 2\pi r\frac{hdh}{dt}$$

If the exponential is replaced with the first term of its series expansion, integrating, and considering $(h/r) = (\Delta L/L_0)$:

$$\frac{\Delta L}{L_0} = \frac{1}{3}\frac{\Delta V}{V} = \left(\frac{6k_2\gamma_{lv}V_0 D\delta C_0}{k_1 RT}\right)^{1/2} r^{-4/3}t^{1/2} \propto r^{-4/3}t^{1/3}$$

The shrinkage due to *solution-precipitation* should be proportional to the one-third power of time and inversely proportional to the four-thirds power of the initial particle size. In addition, with reasonable assumptions as the values for the constants involved, an estimation of the order of magnitude for the sintering-densification rate can be made.